13th International Conference on CANDU Fuel
Holiday-Inn Waterfront Hotel
Kingston, Ontario, Canada, 2016 August 15-18. Paper #70.

MODELLING OF FUEL BUNDLE DEFORMATION UNDER HIGH-TEMPERATURE TRANSIENT CONDITIONS

Zhen Xu, Shouze (George) Xu, Hazen Fan, and Masoud Shams
Fuel Engineering Department, Candu Energy Inc[1]., 2285 Speakman Drive
Mississauga, Ontario, Canada L5K 1B1
(Email of corresponding author: Zhen.Xu@snclavalin.com)

ABSTRACT – CANDU®[2] fuel bundle deforms during operation and under postulated AOO and DBA conditions. Bundle deformations under high-temperature (HT) transient conditions are complex and require many new models to be developed, implemented and tested. Candu Energy has developed a computer program prototype to simulate bundle deformations under AOO and DBA conditions. Some examples of new models include those for dealing with transient conditions, HT thermal loads, inter-element contacts at locations other than spacer pads and bearing pads (i.e., sheath-sheath contacts and sheath-pressure tube (PT) contacts), effects of pre-transient conditions (bundle deformations from normal operation prior to AOOs or DBAs), HT sheath creep, and HT material property changes.
This paper describes an overview of Candu Energy's experience in developing a proprietary computer program, HT version of BOW code (called "BOW-HT" thereafter in this paper) to model fuel bundle deformation under HT transient conditions.

1. Introduction

CANDU fuel bundle deformations under postulated high temperature conditions, including Anticipated Operating Occurrences (AOOs) and Design Basis Accidents (DBAs), are complex and require significant experimental and analytical studies to close the gaps between the requirements and modelling [1]. Of particular interest are the thermal and mechanical loads imposed on the pressure tube (PT) as the fuel elements deform into contact with the PT, and the coolant flow rate through the sub-channels as deforming fuel elements constrict localized flow area, affecting bundle coolability.

1.1 Observed Fuel Bundle Deformations

Fuel bundle deformations were observed during post-irradiation-examination (PIE) of irradiated CANDU power reactor fuel bundles from normal operation, and during out-reactor testing of fuel bundles. Fuel bundles deform as a result of fuel (bundles) string structure responding to various load changes and to support conditions. The bundle deformations include

- lateral deflections of fuel elements (FEs), such as
  - FE thermal bow: FE deflects toward hot side of the sheath (see Figure 1 and Figure 2),
  - FE sag: FE deflects downwards under its own weight due to gravity (illustrated in Figure 3, also see bundle top FEs in Figure 2 and FE#2 and #18 in Figure 4), and
  - FE droop: bottom FEs bend downward at endcaps and upward at bundle midplane (illustrated in Figure 3, also see Figure 2).
- inter-element contacts and FE-PT contacts that affect FE lateral deflections (to form M-shaped or W-shaped FE axial profiles): an evidence for inter-element contact within a fuel bundle during operation is that the "W" shape of FE #2 along the axial direction, shown in Figure 4, is caused by the contact at spacer-pad location (at the bundle midplane) from the intermediate FE right below. FE #2 was at the top

[1] Candu Energy Inc., a Member of the SNC-Lavalin Group
[2] CANDU® (CANada Deuterium Uranium®) is a registered trademark of Atomic Energy of Canada Ltd (AECL), used under exclusive license by Candu Energy Inc.

of the bundle during irradiation (Figure 4). Without FE-FE contacts, an FE axial profile will typically look like those shown in Figure 1, i.e., “C” shaped.

- deformation of endplates (such as dishing, doming, and tilting resulting from neighbouring endplates contacts, shown in Figure 5; and in-plane deformation) and contacts between two neighbouring endplates in a fuel string.
- changes in bundle geometry, such as bundle droop and parallelogramming (which can also cause S-shaped FE axial profile) under NOC, shown in Figure 6; and settling and slumping under postulated high-temperature DBA conditions, shown in Figure 7.
- changes in sub-channel geometry (or sub-channel flow area illustrated in Figure 9); and
- localized fuel-element deformations: such as bamboo shape due to fuel-pellet hour-glassing under NOC, and sheath ballooning under postulated DBA conditions.

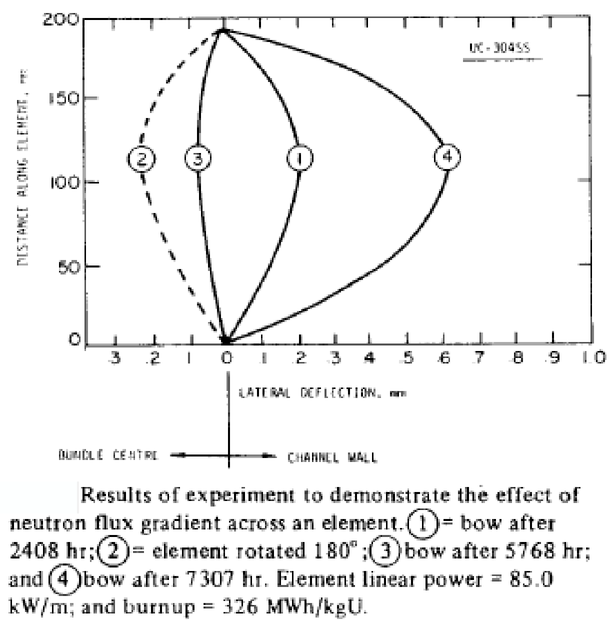

Figure 1 Observed Thermal Bow toward Hot Side of a Fuel Element in a Vertical Fuel Channel, and C Shaped Axial Profiles (from Reference [2])

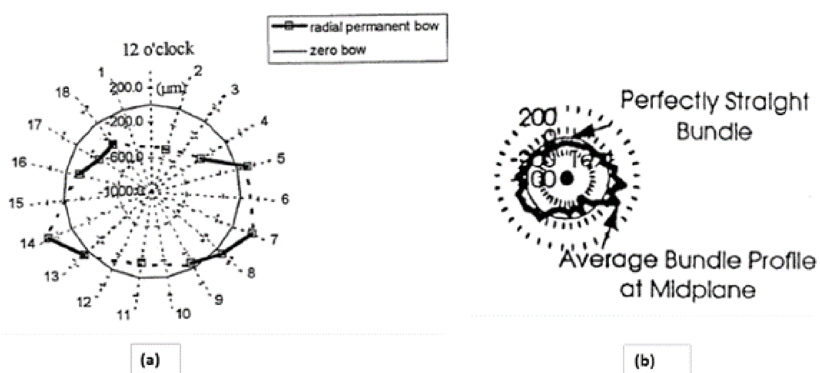

Top FEs sagged (downward deflection), side FEs (near 4 and 5 o’clock, and 7 and 8 o’clock) bowed (outward deflection), bottom FEs (near 6 o’clock) drooped (upward deflection at midspan)

Figure 2 PIE Measured and Darlington 40-Day Endurance Test Observed Outer-Element Profiles at Bundle Midplane Cross Section (from References [3] and [4])

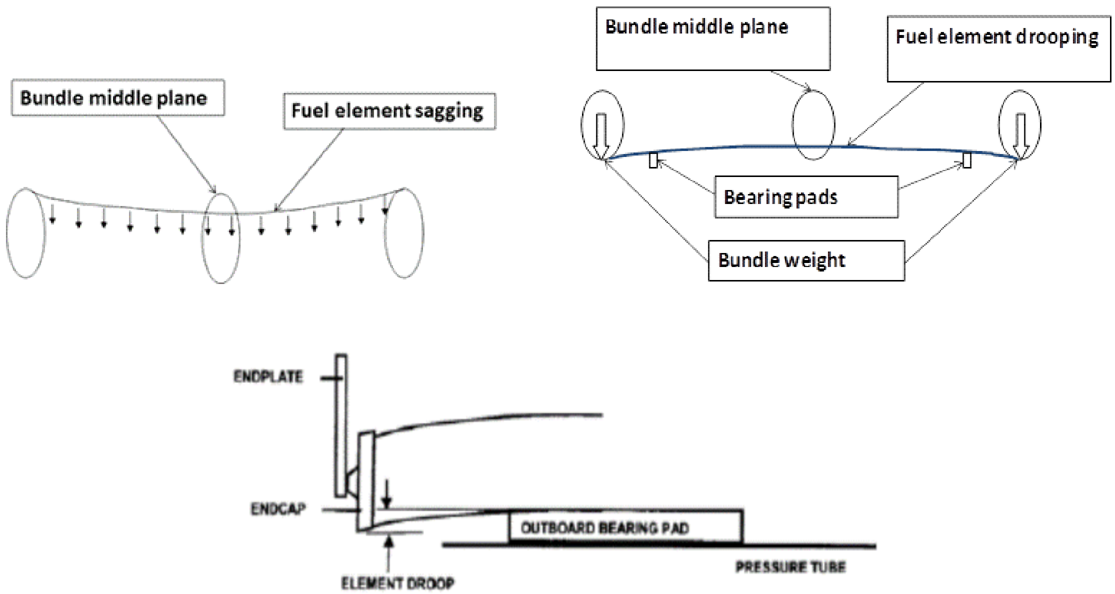

Figure 3 Illustrations of Fuel Element Sagging and Drooping

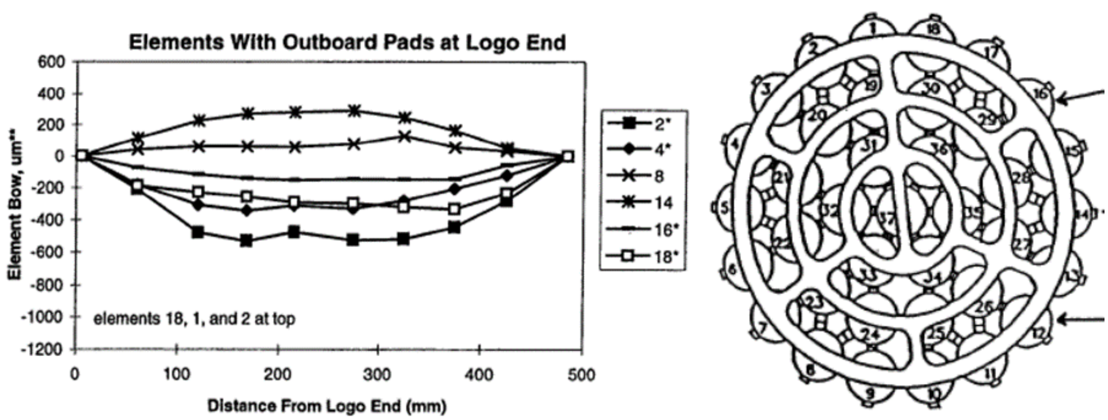

Figure 4 PIE Measured Axial Profiles of Fuel Elements in Intact Irradiated Bundle (from Reference [4])

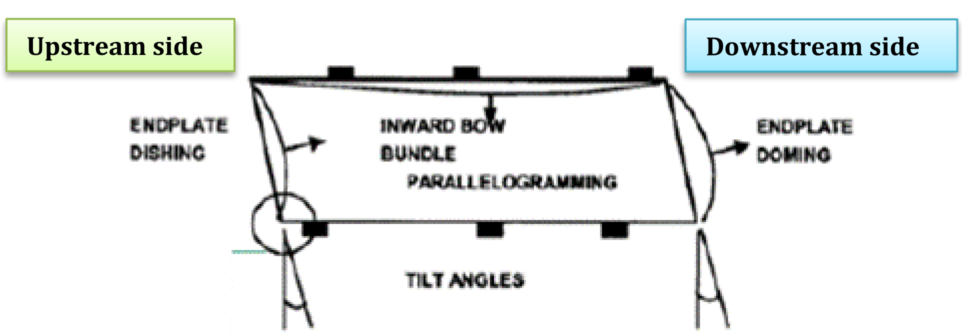

Figure 5 Illustrations for Endplate Dishing, Doming, and Tilting

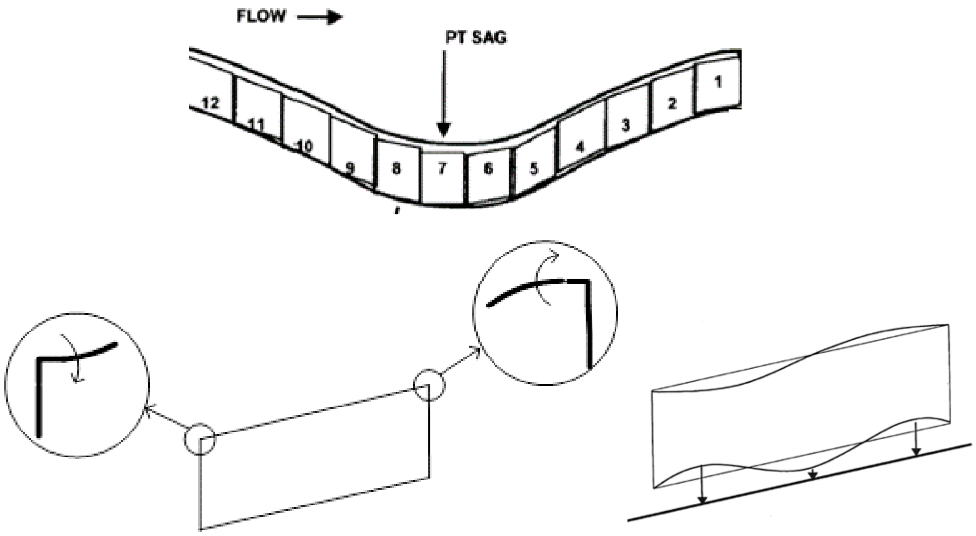

Figure 6 Illustrations for Observed Bundle Parallelogramming, Element S-Shaping and Element M-Shaping in an Aged Fuel Channel

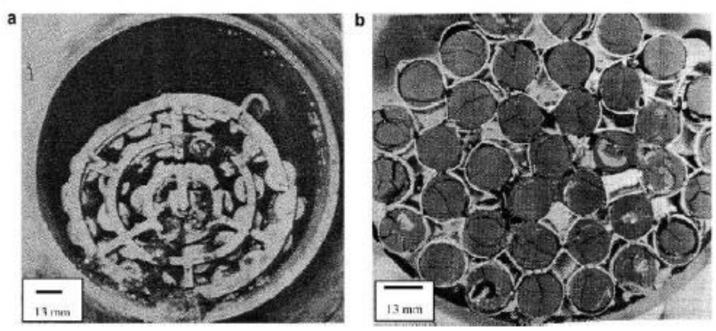

Figure 7 Fuel Bundle Slumping Observed from Very High Temperature Tests (a) Endplate View, (b) View of Bundle Cross Section 30 mm from Endplate (from Reference [5])

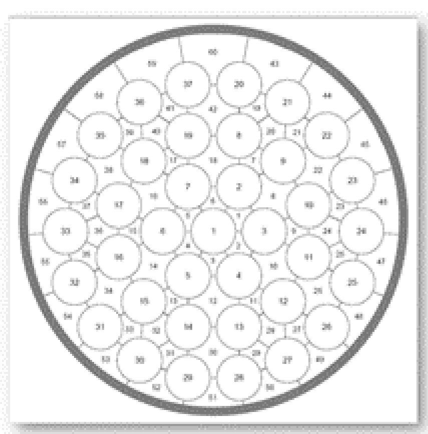

Figure 8 An Illustration of Sub-Channels in a 37-Element Fuel Bundle

1.2 Bundle Deformation Effects on Fuel Performance during a Limited Post-Dryout Operation (PDO)

Some non-LOCA events such as loss of forced circulation and loss of reactivity control may cause limited fuel sheath dryout at full power operation. Under this limited post-dryout conditions, fuel sheath may develop partial dryout patches, heat up locally within the drypatch and trigger temperature-dependent fuel element/bundle deformation mechanisms. An example in locally heating-up caused FE deflections is given in Figure 9, for a deformed experimental FE that was exposed to localized overheating in a test reactor (Reference [6]).

One of the feedbacks from the deformed bundle geometry to fuel performance is that the sub-channel flow areas are changed as a result of bundle deformation, which in turn affects the flow through the sub-channels and hence the local heat transfer between fuel sheath and coolant.

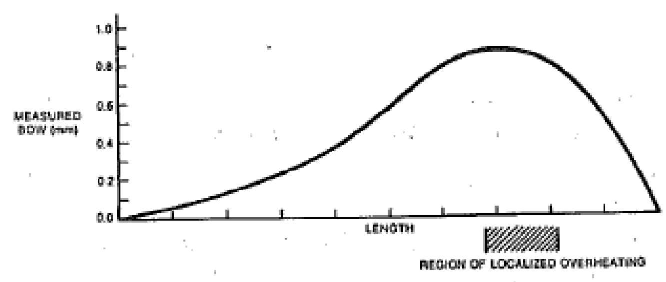

Figure 9 Measured Bows of an Experimental Fuel Element Exposed to Localized Overheating (from Reference [6])

For safety analysis purposes, it is important to understand the extent of the potential fuel post-dryout behaviour and the feedback of fuel bundle deformation to fuel performance [7].

1.3 Bundle Deformation Effects on Coolable Geometry under DBA Conditions

Bundle deformation results are needed in some DBA analyses. For example, bundle coolable geometry during a DBA such as large break LOCA can be assessed based on the predicted deformed bundles in a fuel string.

1.4 Pre-Transient Conditions in AOO and DBA Bundle Deformations

A postulated AOO or DBA can occur any time during a normal operation, and certain amounts of bundle deformations exist prior to the start of an AOO or DBA. Such amounts of bundle deformation are the pre-transient (i.e., initial) conditions for transient bundle deformations under AOO or DBA conditions. Based on observations described in Section 1.1, it can be seen that bundle deformations are quantified using the following parameters:

- displacements (FE deflection, endplate deformations are represented by displacements, and sub-channel geometry is also dependent on FE displacements), and
- contact locations and contact forces (contacts affect displacements of bundle components).

The displacements are vectors not scalars, and the possible contacts can change the directions of displacements; hence initial conditions in bundle deformations are necessary and cannot be ignored. Ignoring initial deformations will change the incremental deformation changes during an HT transient, and thus causes erroneous results in calculations of incremental deformation changes.

When fuel bundle deformations during AOO and DBA are to be analyzed, bundle deformations from NOC must be used as initial conditions (i.e., pre-transient conditions).

1.5 Use of BOW 4.0 to Provide Pre-Transient Conditions

1.5.1 Status of BOW 4.0

BOW 4.0 [8] is a 3rd generation code modelling deformations of all fuel bundles in a fuel string in a CANDU reactor fuel channel under NOC and certain AOO conditions. BOW 4.0 succeeded the previous bundle version BOW 3.0 [9] which succeeded the element version BOW 2.x or earlier version ([6], [10] [11]). Many new models and algorithms were developed and implemented in BOW 4.0 (see Reference [8]). Especially, BOW 4.0 models all bundles in a fuel string inside an aged fuel channel, with bundle-bundle contacts at neighbouring endplates in a fuel string, inter-element contacts, and element-PT contacts. Together with the input parameters from upstream codes and other inputs, BOW 4.0 models the fuel channel ageing effects. The two main effects from fuel channel ageing include:

- Increased radial clearance (due to diametral creep of PT) between outer elements and PT;
- Changes in PT axial support conditions due to PT sagging, which cause fuel bundles to deform into parallelogram shapes.

In addition, BOW 4.0 models operating conditions such as misalignment between two fuel bundles in a fuel string. Description of other models implemented in BOW 4.0 can be found in Reference [8].

1.5.2 Pre-Transient Conditions Using BOW 4.0

BOW 4.0 should be used to get the pre-transient conditions (i.e., initial conditions) when modelling transient bundle deformations, since it has already been developed, verified and validated, documented, and approved for use. The code is available to users[3].

2. Considerations in Modelling of Bundle Deformation during AOOs and DBAs

2.1 Scenarios and Phenomena Considered

Reference [1] describes the required AOO and DBA scenarios to be considered. Due to the space limit, they are not repeated here.

For phenomena, the intended application of a bundle deformation code is covered by the discipline of Fuel and Fuel Channel Thermal-Mechanical Behaviour (FC), and the phenomenon of Bundle Mechanical Deformation (FC12) according to the Technical Basis Document (TBD) developed by CANDU industry. The processes included in the phenomenon FC12 are [1]:

- Bundle slumping due to high temperature creep-sag of individual elements and endplates
- Differential element expansion and fuel element bowing,
- Bundle distortion under axial loads,
- Bundle distortion due to impacts, and
- Wear or dimensional change due to vibration and acoustics, and endplate cracking by fatigue.

Since the mechanism responsible for the last two bullets is independent of high temperature, they were modelled separately in other codes at Candu Energy and not considered in BOW-HT.

There are other FC phenomena affecting fuel temperatures or fuel bundle support conditions which therefore indirectly or directly affect bundle deformation. The relevant FC phenomena include

1) FC1, fission and decay heating
2) FC2, diffusion of heat in fuel
3) FC3, fuel-to-sheath heat transfer
4) FC4, fuel-to-endcap heat transfer
5) FC5, fission gas release to gap and internal pressurization
6) FC6, sheath deformation

[3] External users can contact Candu Energy Code Centre for accessing BOW 4.0.

7) FC8, fuel deformation
8) FC9, sheath oxidation or hydriding
9) FC12, Bundle mechanical deformation
10) FC13, Sheath to coolant and coolant to pressure tube heat transfer
11) FC18, Pressure tube deformation or failure
12) FC21, Element to pressure tube radiative heat transfer
13) FC22, Element or bearing pad to pressure tube contact heat transfer

It is noted that FC1, FC2, FC3, FC4, FC5, FC6, FC8, FC9 are already modelled in the ELOCA code [12] (except sheath hydraiding[4]) for AOO and DBA conditions; FC13, FC18, FC21, and FC22 are already modelled in the CATHENA/TUF [13] code. Since ELOCA and CATHENA/TUF are used in bundle deformation analysis, it is not worthy of the efforts in developing similar models. Rather, the efforts should be focused on developing new and essential models for bundle deformation which are currently not available, and BOW-HT development followed this strategy.

2.2 Modelling Transient Conditions

During a high temperature transient such as large LOCA, the temperatures in a fuel bundle (and fuel elements of the bundle) can change rapidly with time, due to factors such as

- Change in HTS pressure, degraded cooling and increase in fuel temperature;
- Increase in reactor power due to the positive coolant void reactivity feedback before reactor trips (i.e., power pulse for a fuel bundle);
- Change in coolant flow, e.g., flow reversal; and
- Change in cooling conditions, e.g., flow stagnation, loss of inventory or coolant boiling off (voiding), causing portion of some fuel elements to be exposed to the steam.

The transient conditions are modelled as follows,

- Use of ELOCA Results as Input to BOW: a new time loop was added for modelling the transient, and ELOCA calculated fuel temperatures are used as input[5].
- Effect of Degraded Cooling (Change in HTS Pressure): CATHENA or TUF code can be used to provide coolant conditions to ELOCA (for AOO and DBA). The effects of degraded cooling during a transient are accounted for by use of these codes.
- Effect of Power Pulse: The effect of power pulse on fuel temperatures is modelled in ELOCA code, whose temperatures are provided to BOW-HT as input.
- Effect of End Flux Peaking during Coolant Flow Reversal: a flow reversal (e.g., due to RIH break) in large LOCA can cause bundle-coolant contact due to bundle separation and hence end flux peaking. The effect of flux peaking on fuel temperatures is modelled in the FEAT code [15], which can provide temperature increases [16] as inputs to BOW-HT.
- Effect of Cooling Conditions Change (e.g., Steam Cooling): cooling conditions such as steam cooling are much worse than liquid coolant cooling. Fuel behaviour under steam cooling is modelled in ELOCA code, whose temperatures are provided as input to BOW-HT.

2.3 Possible Codes Used in AOO and DBA Bundle Deformation Analysis

Based on the discussion in Section 2.2, computer codes possibly needed for fully analysing fuel bundle deformations under AOO and DBA conditions include RFSP [17], WIMS [18], CATHENA (or TUF) [13], ELESTRES [19], BEAM [20], FEAT [15], BOW [8] [21], ELOCA [12], and BOW-HT, as shown in Figure **10**.

---

[4] Sheath hydriding is not modelled in ELOCA code, however, is modelled in FEED code [14] which may be considered for HT conditions if needed.
[5] An HT transient DBA event such as large LOCA is not expected to cause bundle structural vibration, plus there is a high damping [1].

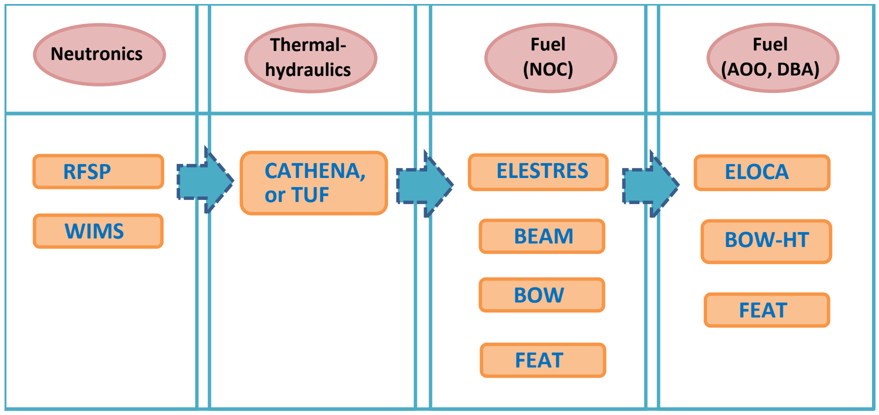

Figure 10 Illustration for Possible Codes Used in Modelling Bundle Deformations under AOO and DBA Conditions

3. Development of BOW-HT for Predicting AOO and DBA Bundle Deformations

Based on the requirements in modelling bundle deformations under AOO and DBA conditions, existing bundle deformation modelling code, BOW 4.0, was assessed to identify gaps in meeting the requirements. Development of HT version of BOW (i.e., BOW-HT) started at Candu Energy a few years ago, which includes developing essential models to calculate bundle deformations under AOO and DBA conditions. Due to the space limit, only brief descriptions of major new models are given below.

- Interface with ELOCA code, for fuel behaviour during the transient and direct use of ELOCA results as input to BOW-HT (hence, many phenomena under AOO and DBA conditions can be modelled using ELOCA and BOW-HT codes).
- Model for HT thermal loads due to irregularly-shaped dry-patches.
- Sheath-sheath contact model and sheath-PT contact model.
- Model to deal with the pre-transient bundle deformation.
- Model for instantaneous plastic bending and HT creep and creep laws (including dislocation creep, diffusional creep and transition creep, and Zr phase change effects).
- Material properties at HT conditions.

The BOW-HT has gone through verification. Validation will start when experimental data are available.

3.1 Interfacing of BOW-HT with ELOCA

Interfacing of BOW-HT with ELOCA was considered first, for the following purposes: a) to model the transient and use ELOCA calculated transient temperatures and other parameters as input to BOW-HT calculations; b) to update thermal loads for use in calculations within BOW-HT.

3.1.1 Governing Equations

A fuel element is considered as a composite beam and modelled with a set of beam finite elements in BOW-HT code. A fuel bundle can be considered as an assembly of connected composite beams. The governing equation for the bundle (i.e., finite-element assembly) can be written as

$$[K]\{u\} = \{P\} \quad (1)$$

where $[K]$ is the global stiffness matrix, $\{u\}$ the general displacement vector; and $\{P\}$ the global load vector.

1) The global stiffness matrix $[K]$ is formed by the grouping of all bundle members (fuel elements, endplate rings and webs): $[K]=\sum_e [K_e]$, where $[K_e]$ is the stiffness matrix for i^{th} beam finite element '*e*'.
2) The global load vector $\{P\}$ contains two parts, $\{P\}=\{P\}^o+\{P\}^c$. $\{P\}^o$ is ordinary load (i.e., gravity load, thermal load and creep load: $\{P\}^o=\sum_e \{P\}^e$, where $\{P\}^e$ is load vector for finite element '*e*'). $\{P\}^o$ can be calculated before Eq. (1) is solved. $\{P\}^c$ is contact load, depending on displacement vector $\{u\}$ and need to be solved simultaneously with $\{u\}$.

3.1.2 Finite-Element Stiffness Matrix

The stiffness matrix has two components: $[K_e]=[K_e^e]+[K_e^g]$. The first term, $[K_e^e]$, is the elastic stiffness matrix and is dependent on the flexural rigidity (*EI*) and torsional rigidity (*GJ*), and are related to temperatures-dependent material properties (Young's modulus E and shear modulus *G*). The second term, $[K_e^g]$, is the geometrical stiffness matrix and is affected by the axial force in the element.

3.1.3 Loads Affecting Fuel-Elements Lateral Deformation

The loads on a fuel element include: a) mechanical loads: lateral loads (e.g., gravity) and axial loads (e.g., hydraulic drag); b) thermal loads: sheath thermal loads, and pellet thermal load; and c) creep load: material creep under mechanical and thermal bending loads cause creep strain differentials over fuel element cross section (hence equivalent bending moment).

Under AOO and DBA conditions, sheath thermal loads and pellet thermal loads change with temperatures.

1) Sheath Thermal Loads in Lateral Directions: $M_x^T=\int_A \alpha_s E_s \Delta T\, r\cos(\theta)\, dA$, where M_x^T is thermal moment in *x* directions (there is a similar moment in *y* direction); E_s is sheath Young's modulus; ΔT is temperature variation over cross section; α_s is sheath thermal expansion coefficient; *A* is sheath cross-sectional area; and (r,θ) are local coordinates for a fuel-element cross section.

2) Sheath Thermal Loads in the Axial Direction: $F_z^T=\int_A \alpha_s E_s \Delta T dA$, where ΔT is the temperature increment with respect to the initial temperature.

3) Pellet Thermal Loads in Lateral Directions: pellet thermal loads include a) pellet bending moment due to neutron flux, and b) drypatch-caused pellet bending (note that drypatches also induce axial thermal strain difference at pellet-sheath interface).

The thermal moments cause bending of the pellet stack, which in turn causes fuel element to bend because of the pellet-sheath interaction (represented by the interaction coefficient, which is always less than 100%). In BOW-HT this pellet-sheath interaction coefficient is *CTF,* the curvature transfer factor, calculated according to the semi-mechanistic model for *REF* since *CTF=REF* (see Reference [21]).

4) Pellet Thermal Loads in the Axial Direction: In the axial direction, the pellet thermal load is in the form of ${}^pF_z^T=\begin{cases} 0 & if \quad \alpha_p\Delta\overline{T}\le g_0 \\ (\alpha_p\Delta\overline{T}-g_0)\overline{E}_p A_p & if \quad \alpha_p\Delta\overline{T}>g_0 \end{cases}$, where $\Delta\overline{T}$ is average pellet temperature; $\overline{E}_p$ is average pellet Young's modulus, g_0 is initial axial gap; and A_p is the area of pellet cross section.

3.2 Modelling Irregular Shaped Dry Patches and other Thermal Loads

Thermal loads due to irregularly-shaped dry-patches (e.g., see Figure 11 for a temperature map, defined by two coordinates in the axial and circumferential directions) were treated in BOW code using new models to perform the thermal load calculation. The temperature distribution within a dry-patch is represented in tabular form (i.e., a digitized temperature map).

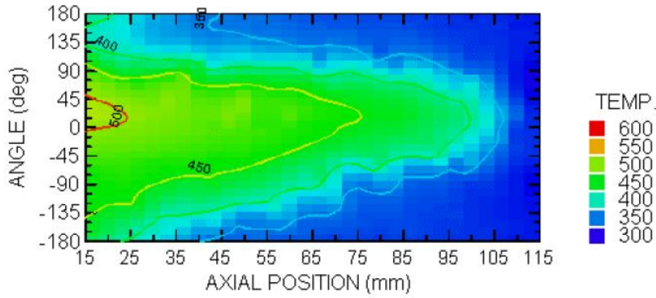

Figure 11 Typical Dry Patch Contour Plot Based on Measurements (from Reference [7])

3.2.1 Re-organizing Raw Data

Test data in a dry patch temperature map often come in mixed sequence, i.e., some with increasing coordinate while others with decreasing coordinate. To use such data in BOW calculations, the raw data were processed first in BOW code.

3.2.2 Calculating Temperatures at Numerical Integration Nodes

When performing numerical integration for the thermal load, the locations of integration nodes used in the BOW code are usually different from measured temperature locations. In BOW code, a model was added to first determine temperatures at the numerical integration points, based on their four neighbouring nodes where the temperatures were measured.

3.3 Models for Sheath-Sheath Contacts and Sheath-PT Contacts

HT conditions can cause more severe bundle deformations, including sheath-sheath contact and sheath-PT contact. The existing models in BOW 4.0 were extended for such purposes and implemented in BOW-HT.

3.3.1 Modelling of Possible Sheath-Sheath Contact or Sheath-PT Contact

Sheath-sheath contact and sheath-PT contact can occur at high temperatures, due to a number of reasons, for example, a) reduction in the element flexural rigidity, b) large creep at high temperatures, and c) reduction in the yield strength.

Sheath-sheath or sheath-PT contacts occur at bundle cross sections where there are no spacer pads or bearing pads. This requires that bundle cross sections at these locations are included in contact modelling for potential contacts, and was done in BOW-HT. The mixed linear complementary formulations of lateral contacts among fuel elements, which are similar to BOW 4.0, are used in BOW-HT.

3.3.2 Updating Bundle Configuration in Contact Algorithms

When direct sheath-sheath contact and sheath-PT contact occur at bundle cross sections where there are no spacers or bearing pads, the contact pair direction may be changed from the initial direction. Hence, the contact pair directions need to be calculated based on deformed element locations, i.e., the bundle configuration needs to be updated in the contact calculations.

3.4 Model for Effects of Pre-Transient (Initial) Conditions

A model was implemented in the BOW-HT to account for the effects of bundle deformations accumulated during normal operation prior to a postulated AOO or DBA event. The initial conditions in bundle deformation are provided using BOW 4.0 simulating the normal operation.

3.5 Model for High-Temperature Plastic Deformation

In BOW-HT, models for instantaneous plastic bending of fuel–elements and of endplates were developed and implemented. In addition, the creep deformation models were extended to HT conditions and ELOCA 2.2 creep law was implemented (note that the target applications of BOW 3.0 and BOW 4.0 did not include conditions where sheath temperatures exceed the Zircaloy $\alpha \rightarrow (\alpha+\beta)$ phase-change temperature).

The ELOCA creep law is the micro-structural transient creep model developed initially by Sills and Holt [22] is used to describe the HT creep behaviour of Zircaloy sheathing. The sheath stress and temperature transient occurred under HT AOO and DBA conditions will 1) cause significant changes in Zircaloy grain size, 2) cause significant changes in dislocation density, and 3) can trigger the $(\alpha \rightarrow \beta)$ phase change.

These micro-structural changes occur continuously during a HT transient (e.g., large LOCA) and have a strong effect on the Zircaloy creep behaviour. As the ELOCA creep law accounts for changes in sheath microstructure, manufacturing differences between sheaths affecting anisotropy, grain size, and dislocation structure can be explicitly represented. The total creep rate at any time during the transient is equal to the sum of the separate components (dislocation creep rate, diffusion creep rate, and transition strain rate).

3.6 Material Properties at HT conditions

There are a number of material properties that are temperature-dependent (e.g., Young's modulus, shear modulus, thermal expansion coefficient, and yield strength etc. for Zircaloy and for Inconel materials). Such properties require updating when local temperatures change. This was done in BOW-HT.

4. Illustrations for BOW-HT Capabilities

4.1 BOW-HT Models for Different Bundle Structures

Different bundle designs were modelled in BOW-HT during the testing of the code, which include the 3-element bundle, 28-element bundle, 37-element bundle, and 43-element bundle, see Figure 12.

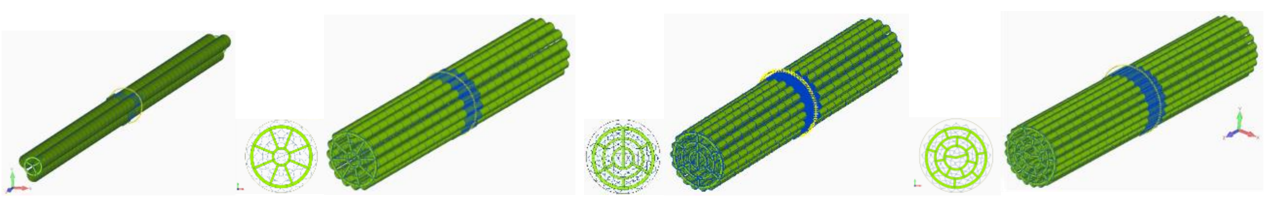

Figure 12 Different Bundle Structures Modelled Using BOW Code (from Left to Right: 3-Element, 28-Element, 37-Element and 43-Element Bundles)

4.2 Illustration for Heated Fuel-Element Elongation and Bundle-Bundle Contact through Endplates

BOW-HT was tested for a case where 3 bundles (37-element bundles) are in a fuel string (Figure 13). The top fuel element #6 in the middle bundle is heated uniformly in full circumference 540°C (see Figure 14). All other elements (in middle bundle, upstream bundle, downstream bundle) are at 320°C uniformly.

Figure 13 A Test Case Containing Three Bundle Fuel String

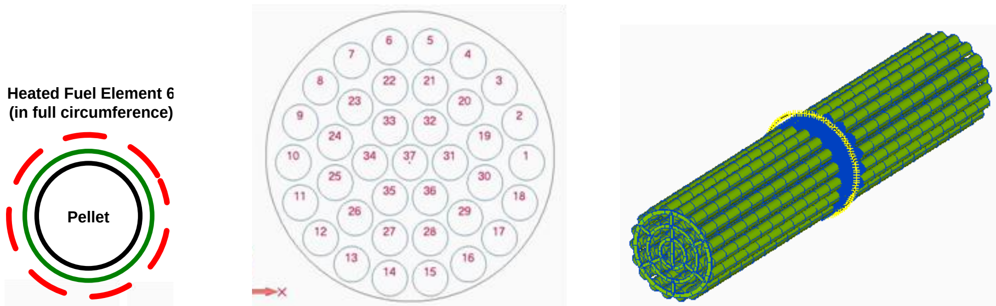

Figure 14 BOW-HT Model to Illustrate the Test Case (Heated Element 6 in the Middle Bundle of a 3-Bundle String)

The heated element elongates due to thermal expansion (left in Figure 15), which affects both axial neighbouring bundles in the fuel string, i.e., upstream bundle and downstream bundle. The bundle-bundle contact through endplates of neighbouring bundles are illustrated in Figure 15, where the corresponding fuel elements (#6) in the upstream bundle and downstream bundle are pushed-in because of the elongation of element #6 in the middle bundle. The effects of such elongation propagate in the fuel string through endplates contacts and endplates deformations. This example shows that even one fuel element elongation affects not only the deformations of other elements in the same bundle, but also the deformations of fuel elements in upstream and downstream bundles.

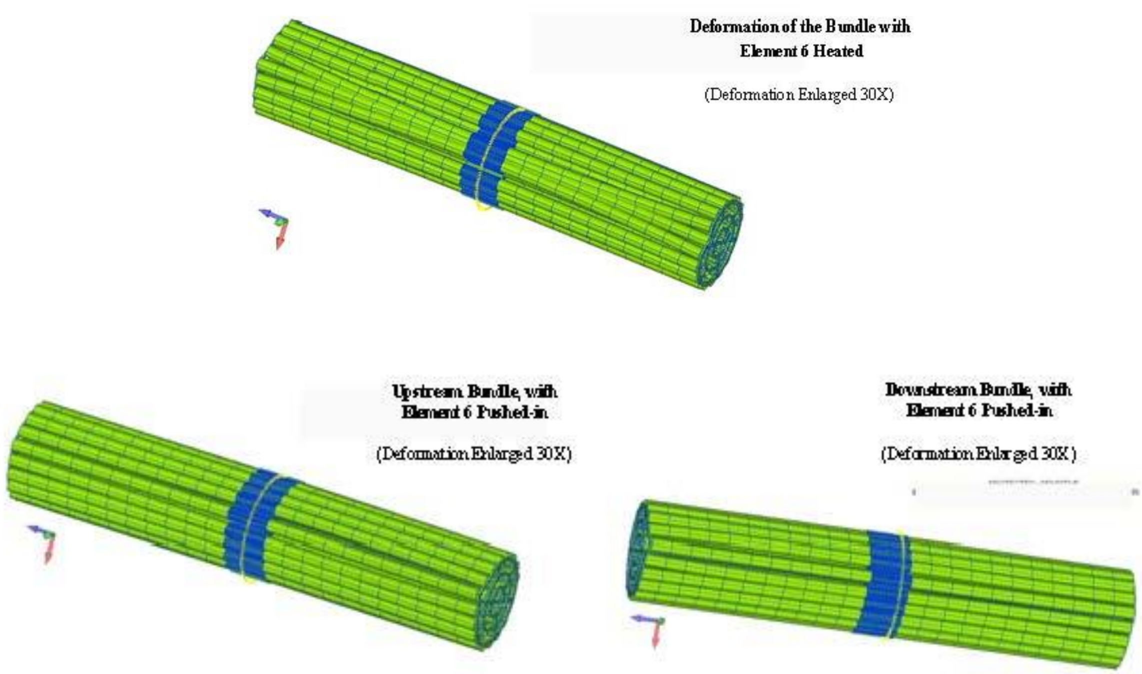

Figure 15 BOW-HT Calculations to Illustrate Elongated Heated Element 6 (Top), Upstream Bundle with Element 6 Pushed-in (Left), and Downstream Bundle with Element 6 Pushed-in (Right)

4.3 Illustration for Sheath-Sheath Contacts under HT Conditions and Sub-Channel Flow Area Changes

In the next test case, a single bundle in a PT is considered. Young's modulus is set to a small value to see the effect of high-temperatures caused FE flexural rigidity reduction on bundle deformation.

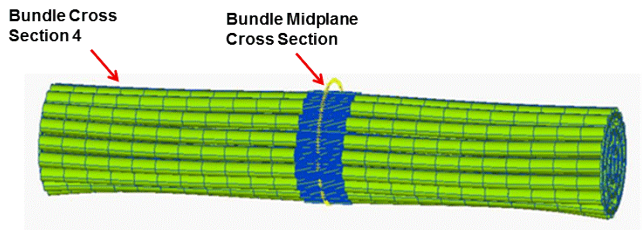

Figure 16 Bundle Cross Sections for Bundle Deformation Output

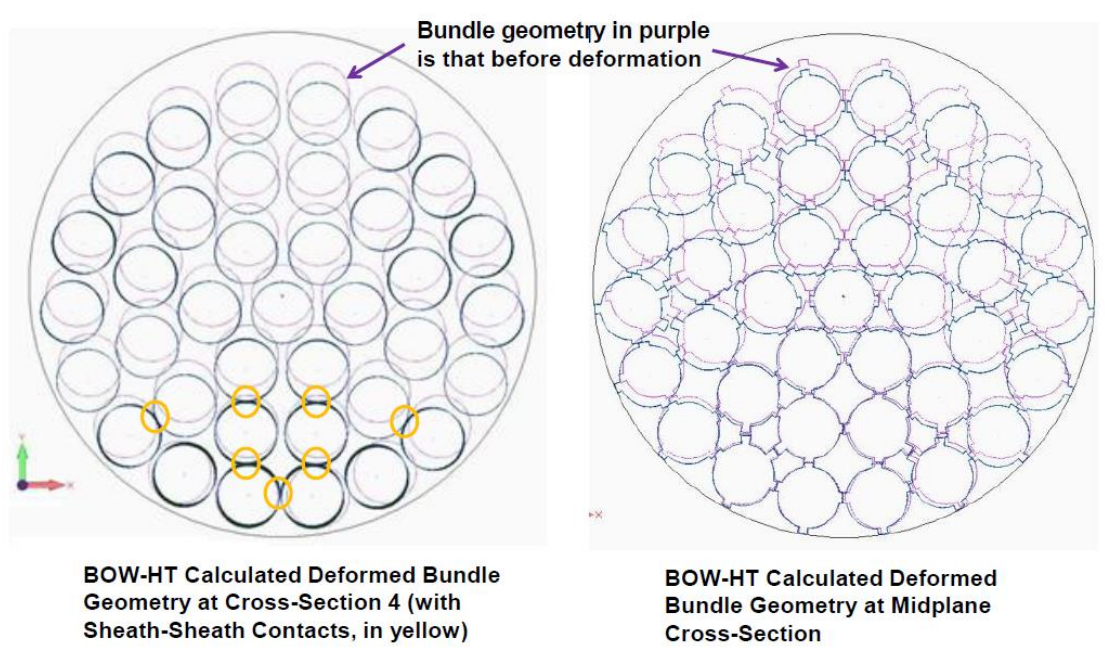

Figure 17 BOW-HT Predicted Sheath-Sheath Contacts in Deformed Cross Sections 4 (Left) and Bundle Midplane (Right) of a 37-Element Bundle

The BOW-HT results show that there are bundle deformations under such conditions and many sheath-sheath contacts occur at bundle cross section 4 (shown in Figure 17). At the bundle midplane, there are also bundle deformations. It clearly shows that as a result of the bundle deformations, the sub-channel flow areas also changed.

4.4 Illustration for Fuel Bundle Slumping

The BOW code was tested for bundle slumping modelling capability in the past. As shown in Figure 18, the calculated bundle cross sectional profile at ¼ bundle length shows slumping for very high temperature conditions (above 1400°C) (right figure). An experimentally observed bundle cross section at very high temperature is shown in the middle figure.

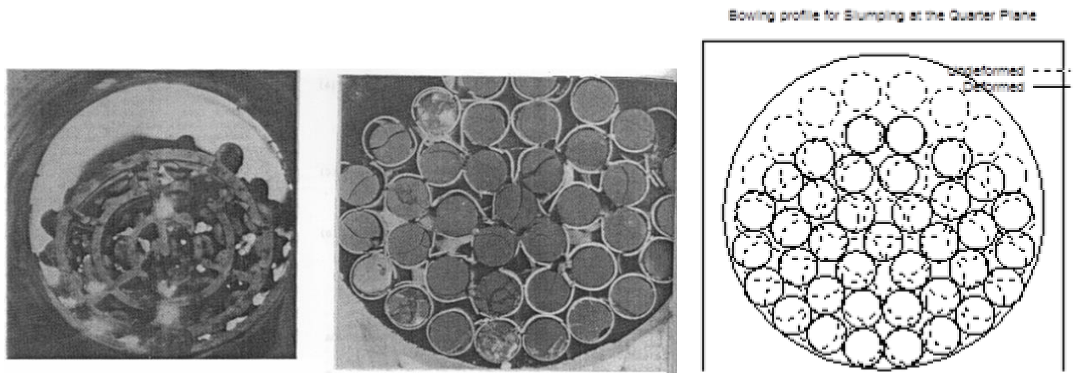

Figure 18 Illustration for BOW Predicted Bundle Slumping (at ¼ Bundle Cross Section), in Comparison with Experimental Observation

5. Case Study

5.1 Case 1: Fuel-Sheath Deflections Caused by Dry-Patches

In Case 1, simply-supported sheath with a dry-patch near one end is considered. The dry-patch angular location and axial location on fuel sheath are given in Figure 19. Inside the dry-patch sheath temperature is higher than outside the dry-patch and temperature difference is ΔT=250 °C.

BOW-HT calculation results are compared with analytical solutions and they are found to be almost identical to analytical solutions, see Figure 19.

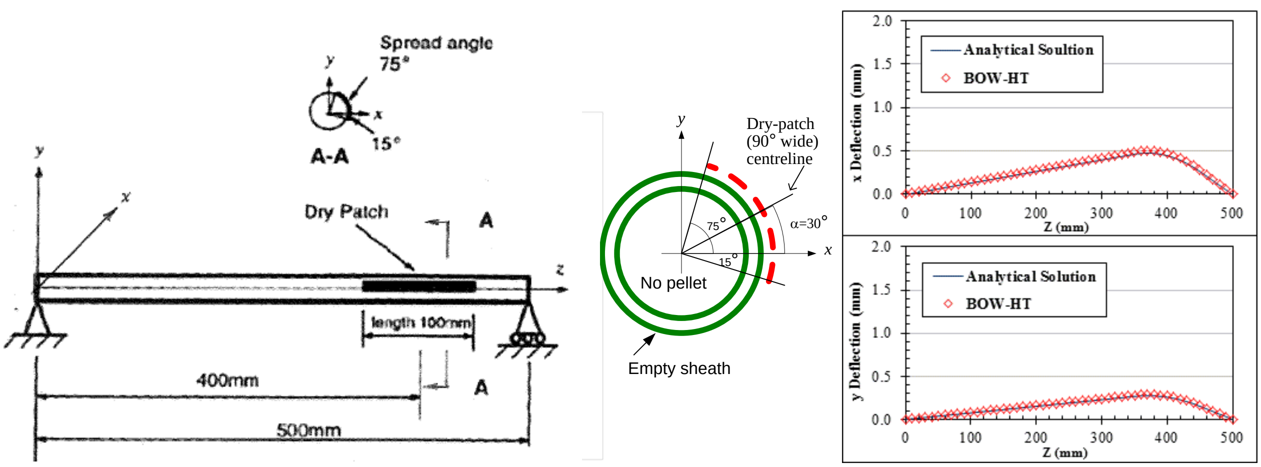

Figure 19 Simply-Supported Sheath with a Dry Patch: Comparisons of BOW-HT Calculations with Analytical Solutions

5.2 Case 2: Three-Element Structure Heating Tube Deflections Caused by Dry-Patches

Case 2 involves a 3-element test bundle structure where only one element was heated and two dry-patches formed on this heating tube. Temperatures from the test measurement are used as input to BOW-HT and bundle deformations were calculated using BOW-HT. Both the temperature maps in the dry-patches on the heating tube and the deformations of the heating tube are shown in Figure 20.

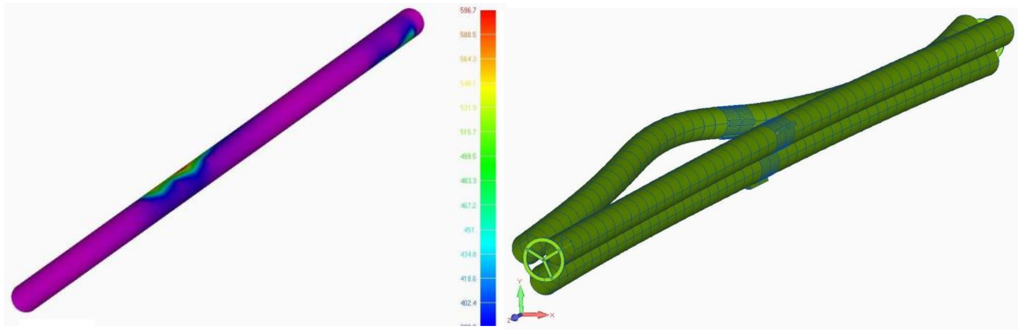

Figure 20 Two Dry-Patches on Heating Element of a 3-Element Test Bundle Structure and Corresponding Deformations Calculated Using BOW-HT (Deformation Enlarged 40x for Better View)

The BOW-HT calculations were compared with the measurements and it is found there is an overall good agreement between BOW-HT calculations and measurements.

6. Conclusions

The prototype BOW-HT has been developed at Candu Energy and test results show that this prototype has the capabilities in modelling required phenomena and providing required output parameters for bundle deformations under AOO and DBA conditions, especially, the prototype can model the irregular-shaped dry-patches caused fuel element thermal bow, the inter element contacts that cause sheath-sheath contacts, the element-PT contacts that cause sheath-PT contacts, bundle-bundle contacts in a fuel string through endplates that cause localized endplates contacts, and bundle slumping under very high temperatures.

7. Acknowledgement

Authors thank Liping Lai and Gong Cheng for their extensive efforts and contributions in development of the BOW-HT; and Fred Huang for providing analysis requirements and analysis conditions.

8. References

[1] S. (G.) Xu, Z. Xu, H. Fan, and T. Nitheanandan, "Modelling of Fuel Bundle Deformation at High Temperatures: Requirements, Models and Steps for Consideration", Proc. 11th International Conference on CANDU Fuel, Niagara Falls, Ontario, Canada, 2010 October 17-20.

[2] J. Veeder and M. Schankula, "Bowing of Pelletized Fuel Elements: Theory and In-Reactor Experiments", Nuclear Engineering and Design, v.29 (1974), pp. 167-179.

[3] D. Dennier, A.M. Manzer, and E. Kohn, "Characteristics of CANDU Fuel Bundles that Caused Pressure Tube Fretting at the Bundle Midplane", 16th CNS Annual Conference (Vol. 2), Saskatoon, Saskatchewan, Canada, June 4-7, 1995.

[4] D. Dennier, A.M. Manzer, M.A. Ryz, and E. Kohn, "Element Bow Profiles from New and Irradiated CANDU Fuel Bundles", Proceedings of 17th Canadian Nuclear Society Annual Conference (vol. 2), Fredericton, New Brunswick, Canada , June 9-12, 1996.

[5] E. Kohn, G.I. Hadaller, R.M. Sawala, G.H. Archinoff, and S.L. Wadsworth, "CANDU Fuel Deformation during Degraded Cooling (Experimental Results)", 6th Annual CNS Conference, Ottawa, Canada, June 3-4, 1985, Canadian Nuclear Society, Toronto, pp.16.39-16.45.

[6] M. Tayal, "Modelling the Bending/Bowing of Composite Beams such as Nuclear Fuel: the BOW Code." Nuclear Engineering and Design, v. 116 (1989), pp. 149-159.

[7] H.Z. Fan, H. Liu, A. Ranger and S.G. Xu, "Assessment of Fuel Element Patchy Dryout and Bowing in Fuel Bundle", 10th CNS International Conference on CANDU Fuel, Ottawa, Ontario, 2008 October 5-8.

[8] S. (G.) Xu, G. Cheng, Z. Xu, D. Wen, and S. Yu, "BOW 4.0: Modeling Deformations of Fuel String with Channel Ageing Effects", 11th CNS International Conference on CANDU Fuel, Niagara Falls, Ontario, 2010 October 17-20.

[9] S.G. Xu, Z. Xu, S.D. Yu, M. Tayal, L. Lai, and B. Wong, "BOW Code Development; Modelling of In-Reactor Bundle Deformation", Proceedings of 9th CNS International Conference on CANDU Fuel, Belleville, Ontario, Canada, 2005 September 19.

[10] S.D. Yu, M. Tayal, P.N. Singh, "Improvements, Verifications, and Validations of the BOW Code", 4th International Conference on CANDU Fuel, Pembroke, Ontario, Oct 1-4, 1995, v.2, Canadian Nuclear Society, Toronto.

[11] S.D. Yu, M. Tayal, and Z. Xu, "Creep Bowing in CANDU Fuel: Modelling and Applications", 5th International Conference on CANDU Fuel, Toronto, Ontario, September 21-25, 1997, v.1, pp. 363-375, Canadian Nuclear Society, Toronto.

[12] A.F. Williams, "The ELOCA Fuel Modelling Code: Past, Present and Future", Proc. of 9th International Conference on CANDU Fuel, Belleville, Ontario, Canada, 2005 September.

[13] B.N. Hanna, "CATHENA: A Thermalhydraulic Code for CANDU Analysis", Nuclear Engineering and Design 180 (1998) 113-131.

[14] L. Lai, Z. Xu, Q. Jiang and G. Cheng, "FEED 1.6: Modelling of Hydrogen Diffusion and Precipitation in Fuel Bundle Zircaloy Components", Proc. of 11th International Conference on CANDU Fuel, Niagara Falls, Ontario, Canada, 2010 October 17-20.

[15] Q. Jiang, L. Lai, Z. Xu, and U.K. Paul, "FEAT 4.1: Modelling of Sheath Oxidation and Heat Flow in CANDU Fuel Elements", Proc. of 11th International Conference on CANDU Fuel, Niagara Falls, Ontario, Canada, 2010 October 17-20.

[16] Z. Xu, Q. Jiang, L. Lai, and M. Shams, "Analysis of Fuel End-Temperature Peaking", 12th International Conference on CANDU Fuel Holiday-Inn Waterfront Hotel, Kingston, Ontario, Canada, 2013 September 15-18.

[17] B. Rouben, "RFSP-IST, the Industry Standard Tool Computer Program for CANDU Reactor Core Design and Analysis", Proceedings of the 13th Pacific Basin Nuclear Conference, Shenzhen, China, 2002 October 21-25.

[18] J.D. Irish and S.R. Douglas, "Validation of WIMS-IST", Proceedings of the 23rd Annual Conference of the Canadian Nuclear Society, Toronto, Ontario, Canada, 2002 June 2-5.

[19] G.G. Chassie, Q. Jiang, H. Liu, M. Tochaie and Z. Xu, "ELESTRES 2.1 Computer Program for High-Burnup CANDU Fuel Performance Analysis", Proc. of 11th International Conference on CANDU Fuel, Niagara Falls, Ontario, Canada, 2010 October 17-20.

[20] G. Cheng, S. (G.) Xu, Z. Xu and U.K. Paul, "BEAM 1.7: Development for Modelling Fuel Element and Bundle Buckling Strength", Proceedings of 11th International Conference on CANDU Fuel, Niagara Falls, Ontario, 2010 Oct 17-20.

[21] S.(G,) Xu and Z. Xu, "Relationship Established between two Important Parameters Used to Simulate on-Power Bundle Deformation", Proceedings of 10th CNS International Conference on CANDU Fuel, Ottawa, Canada, 2008 October 5-8.

[22] H.E. Sills and R.A. Holt, "Predicting High Temperature Transient Deformation from Microstructural Models", 4th International Conference of Zirconium in the Nuclear Industry, Stanford-upon-Avon, 1978.